

Supporting Information:

Eliminating the dication-induced intersample chemical-shift variations for NMR-based biofluid metabonomic analysis

Limiao Jiang,^{a,b} Jing Huang^a, Yulan Wang^a and Huiru Tang^{*a}

^a State Key Laboratory of Magnetic Resonance and Atomic and Molecular Physics, Centre for Biospectroscopy and Metabonomics,

Wuhan Center for Magnetic Resonance, Wuhan Institute of Physics and Mathematics, Chinese Academy of Sciences, Wuhan, 430071, P.R.

China. ^b Graduate University of the Chinese Academy of Sciences, Beijing, 100049, P.R. China

E-mail: Huiru.tang@wipm.ac.cn; Fax: +86-27-87199291; Tel: +86-27-87198430

List of supporting Tables and Figures:

Table.S1 Ca²⁺ and Mg²⁺ concentrations in rat (n=9), mouse (n=9) and human urine (n=12).

Fig.S1 ¹H NMR spectra (δ 2.40-2.74) for rat urine samples (n=10) treated with phosphate buffer (A), with buffer followed with adjusting pH to 7.40 ± 0.03 (B). Dotted insets were vertically expanded 16 times. DMA, dimethylamine; 2-OG, 2-oxoglutarate; Ha and Hb, highfield and lowfield signals of citrate.

Fig.S2 ¹H NMR spectra (δ 2.40-2.74, δ 3.55-3.74) for rat urine samples (n=10) treated with phosphate buffer (A), with K₂EDTA reaching final concentration of 34.4 mM followed with phosphate buffer, and adjusting pH to 7.41 ± 0.02 (B). Free EDTA signals (around δ 3.64) in B indicated that all Ca²⁺ and Mg²⁺ were chelated. Dotted insets were vertically expanded 8 or 16 times. DMA, dimethylamine; 2-OG, 2-oxoglutarate; Ha and Hb, highfield and lowfield signals of citrate.

Fig.S3 Effects of sample treatments on sample pH for rat urine samples (n=10). U: with no treatment; A': treated with K₂EDTA addition and followed by buffering; A and B were same as in Figure S2.

Fig.S4 ¹H NMR spectra (δ 2.40-2.74) for mouse urine with different final KF concentration.

Fig.S5 Effects of KF addition on mouse urine sample pH (\blacktriangle), signal-to-noise ratio (SNR, \blacksquare) and intersample variations ($\Delta \delta$) in the chemical shifts of citrate resonances. Ha (\bullet) and Hb (\blacksquare) are the highfield ($\sim \delta$ 2.52) and lowfield ($\sim \delta$ 2.65) protons from CH₂ moieties of citrate. Relative SNR were calculated against the sample having no KF addition with the signal region of δ 3.26-3.29 (CH₃ signal of TMAO) and the noise region of δ -2 to δ -5.

Fig.S6 ¹H NMR spectra (δ 2.50-2.75) for human urine with different final KF concentration.

Fig.S7 Effects of KF addition on human urine sample pH (\blacktriangle), signal-to-noise ratio (SNR, \blacksquare) and intersample variations ($\Delta \delta$) in the chemical shifts of citrate resonances. Ha (\bullet) and Hb (\blacksquare) are the highfield ($\sim \delta$ 2.52) and lowfield ($\sim \delta$ 2.65) protons from CH₂ moieties of citrate. Relative SNR were calculated against the sample having no KF addition with the signal region of δ 3.00-3.10 (CH₃ signal of creatinine) and the noise region of δ -2 to δ -5.

Fig.S8 ¹H NMR spectra (δ 2.40-2.74, δ 3.55-3.74) for rat urine samples (n=9) treated with phosphate buffer (A), with KF reaching final concentration of 159.5 mM KF followed with phosphate buffer (B) and with K₃EDTA reaching final concentration of 31.9 mM followed with phosphate buffer (C).

Fig.S9 Effects of sample treatments on sample pH (a) and signal-to-noise ratio (SNR) (b) for rat urine samples (n=9) which was calculated from the signal region of δ 2.42-2.47 (γ -CH₂ signal of 2-oxoglutarate) and noise region from δ -2 to δ -5. SNR data were normalized to that from samples treated with only phosphate buffer (mean \pm sd). U: with no treatment; A-C were same as in Figure S8.

Fig.S10 ¹H NMR spectra (δ 2.40-2.74, δ 3.55-3.74) for mouse urine samples (n=9) treated with phosphate buffer (A), with KF reaching final concentration of 71.6 mM followed with phosphate buffer (B) and with K₃EDTA reaching final concentration of 7.2 mM followed with phosphate buffer (C).

Fig.S11 Effects of sample treatments on sample pH (a) and signal-to-noise ratio (SNR) (b) for mouse urine samples (n=9) which was calculated from the signal region of δ 3.26-3.29 (CH₃ signal of TMAO) and noise region from δ -2 to δ -5. SNR data were normalized to that from samples treated with only phosphate buffer (mean \pm sd). U: with no treatment; A-C were same as in Figure S10.

Fig.S12 ¹H NMR spectra (δ 2.50-2.75, δ 3.55-3.74) for human urine samples (n=10) treated with phosphate buffer (A), with KF reaching final concentration of 81.2 mM followed with phosphate buffer (B), with KF reaching final concentration of 120.7 mM followed with phosphate buffer (C), with K₃EDTA reaching final concentration of 13.0 mM followed with phosphate buffer (D) and with KF reaching final concentration of 120.7 mM followed with phosphate buffer and with K₃EDTA reaching final concentration of 6.0 mM (E). These 10 human urine samples included nine adults and one 14-day-old new born baby.

Fig.S13 Effects of sample treatments on sample pH (a) and signal-to-noise ratio (SNR) (b) for human urine samples (n=10) which was calculated from the signal region of δ 3.00-3.10 (CH₃ signal of creatinine) and noise region from δ -2 to δ -5. SNR data were normalized to that from samples treated with only phosphate buffer (mean \pm sd). U: with no treatment; A-E were same as in Figure S12.

Fig.S14 ¹H NMR spectra (δ 2.50-2.75, δ 3.50-3.72) for one 28-month-old baby and one 5-month-old baby, A-E were same as in Figure S12.

Fig. S15 Schematic flow chart for the improved urine sample preparation protocol based on KF additon (using rat urine as examples). PB, phosphate buffer. ^a details are described in the validation section for different urines.

Fig. S16 Schematic flow chart of improved urine sample preparation methods using EDTA-d12 chelation. PB, phosphate buffer. ^a details are described in the validation section for different urines.

Table S1 Ca²⁺ and Mg²⁺ concentrations in rat (n=9), mouse (n=9) and human urine (n=12)

	Concentration/mM ^a		
	Ca ²⁺	Mg ²⁺	Mg ²⁺ + Ca ²⁺
rat urine (n=9)	7.41 ± 3.48	3.02 ± 1.41	10.44 ± 4.88
mouse urine (n=9)	1.03 ± 0.34	2.65 ± 1.20	3.68 ± 1.45
human urine (n=12)	0.87 ± 0.52	0.80 ± 0.59	1.67 ± 0.85

^a mean ± sd.

Fig. S1

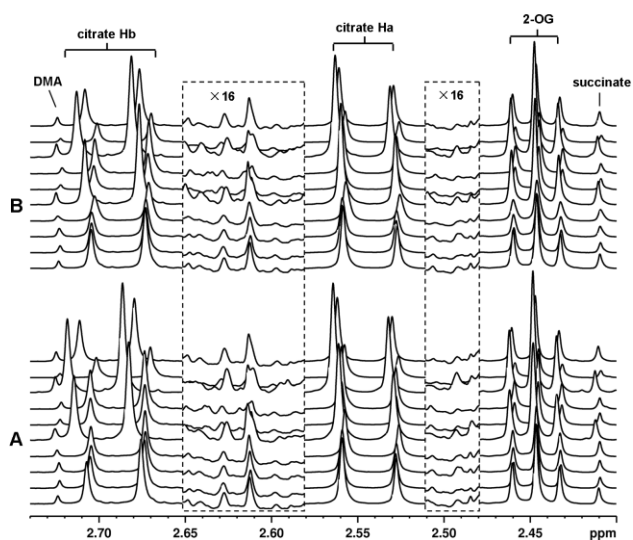


Fig. S1 ¹H NMR spectra (δ 2.40-2.74) for rat urine samples (n=10) treated with phosphate buffer (A), with buffer followed with adjusting pH to 7.40 ± 0.03 (B). Dotted insets were vertically expanded 16 times. DMA, dimethylamine; 2-OG, 2-oxoglutarate; Ha and Hb, highfield and lowfield signals of citrate.

Fig. S2

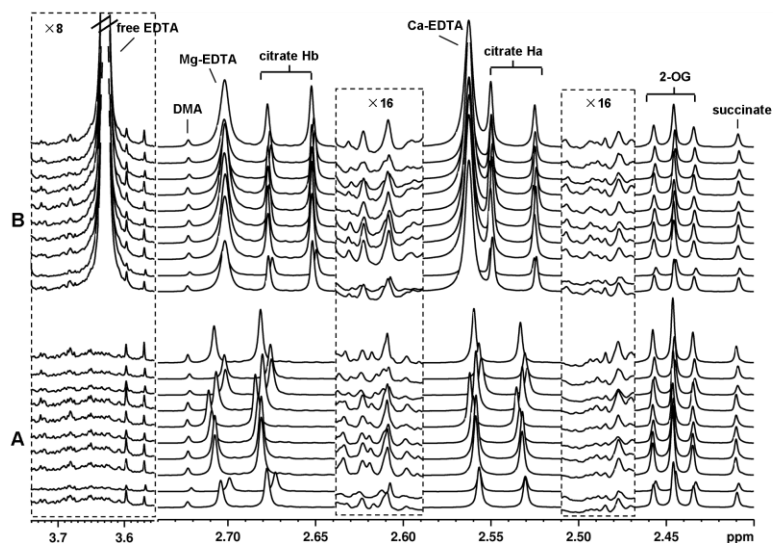


Fig. S2 ^1H NMR spectra (δ 2.40-2.74, δ 3.55-3.74) for rat urine samples ($n=10$) treated with phosphate buffer (A), with K_2EDTA reaching final concentration of 34.4 mM followed with phosphate buffer, and adjusting pH to 7.41 ± 0.02 (B). Free EDTA signals (around δ 3.64) in B indicated that all Ca^{2+} and Mg^{2+} were chelated. Dotted insets were vertically expanded 8 or 16 times. DMA, dimethylamine; 2-OG, 2-oxoglutarate; Ha and Hb, highfield and lowfield signals of citrate.

Fig. S3

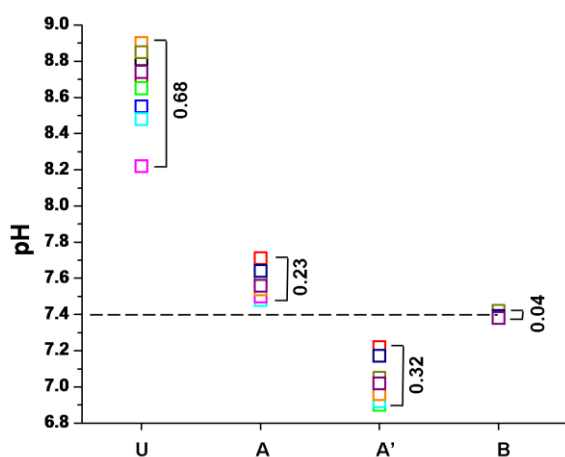


Fig. S3 Effects of sample treatments on sample pH for rat urine samples (n=10). U: with no treatment; A': treated with K_2EDTA addition and followed by buffering; A and B were same as in Figure S2.

Fig. S4

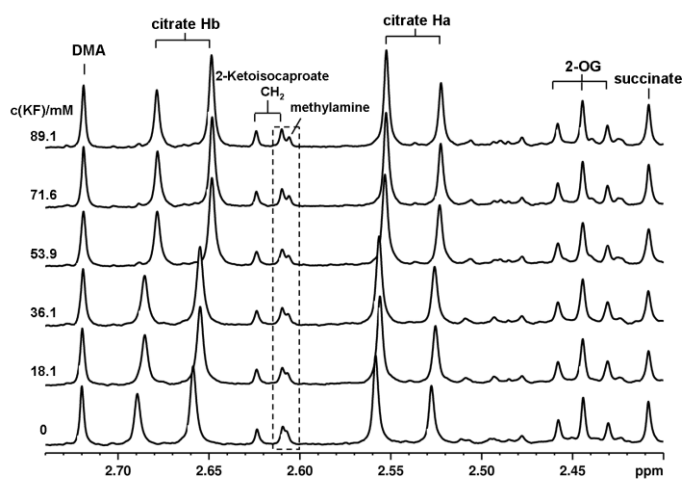


Fig. S4 ¹H NMR spectra (δ 2.40-2.74) for mouse urine with different final KF concentration.

Fig. S5

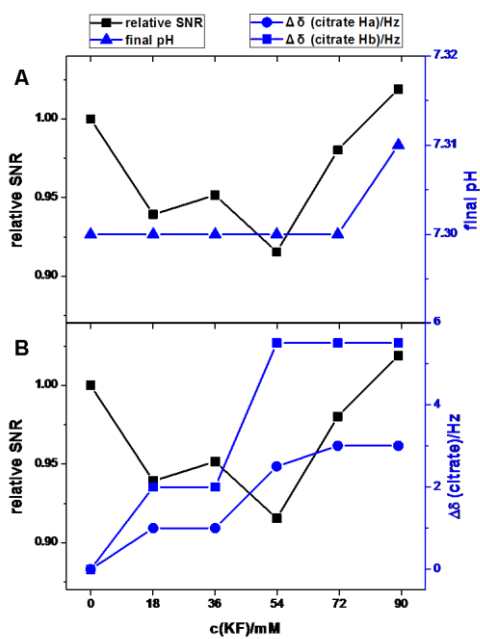


Fig. S5 Effects of KF addition on mouse urine sample pH (\blacktriangle), signal-to-noise ratio (SNR, \blacksquare) and intersample variations ($\Delta\delta$) in the chemical shifts of citrate resonances. Ha (\bullet) and Hb (\blacksquare) are the highfield ($\sim\delta$ 2.52) and lowfield ($\sim\delta$ 2.65) protons from CH_2 moieties of citrate. Relative SNR were calculated against the sample having no KF addition with the signal region of δ 3.26-3.29 (CH_3 signal of TMAO) and the noise region of δ \square -2 to δ \square -5.

Fig. S6

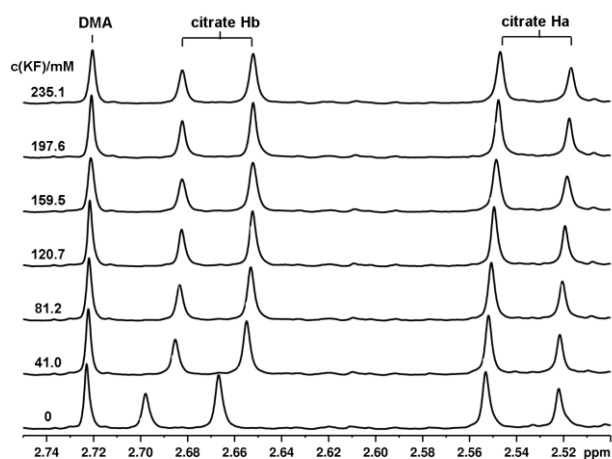


Fig. S6 ¹H NMR spectra (δ 2.50-2.75) for human urine with different final KF concentration.

Fig. S7

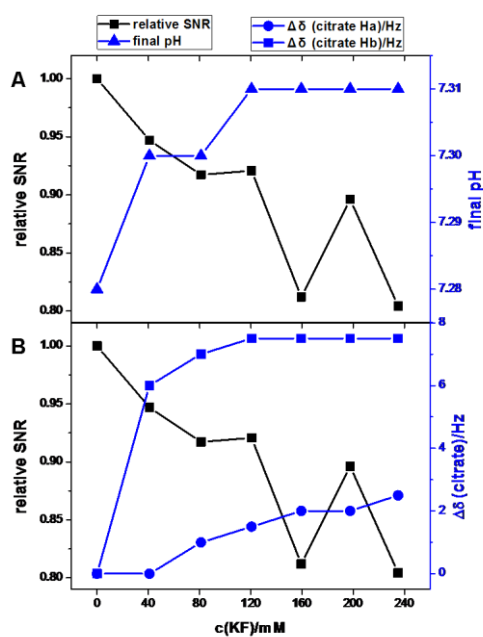


Fig. S7 Effects of KF addition on human urine sample pH (\blacktriangle), signal-to-noise ratio (SNR, \blacksquare) and intersample variations ($\Delta\delta$) in the chemical shifts of citrate resonances. Ha (\bullet) and Hb (\blacksquare) are the highfield ($\sim\delta 2.52$) and lowfield ($\sim\delta 2.65$) protons from CH_2 moieties of citrate. Relative SNR were calculated against the sample having no KF addition with the signal region of $\delta 3.00$ - 3.10 (CH_3 signal of creatinine) and the noise region of $\delta -2$ to $\delta -5$.

Fig. S8

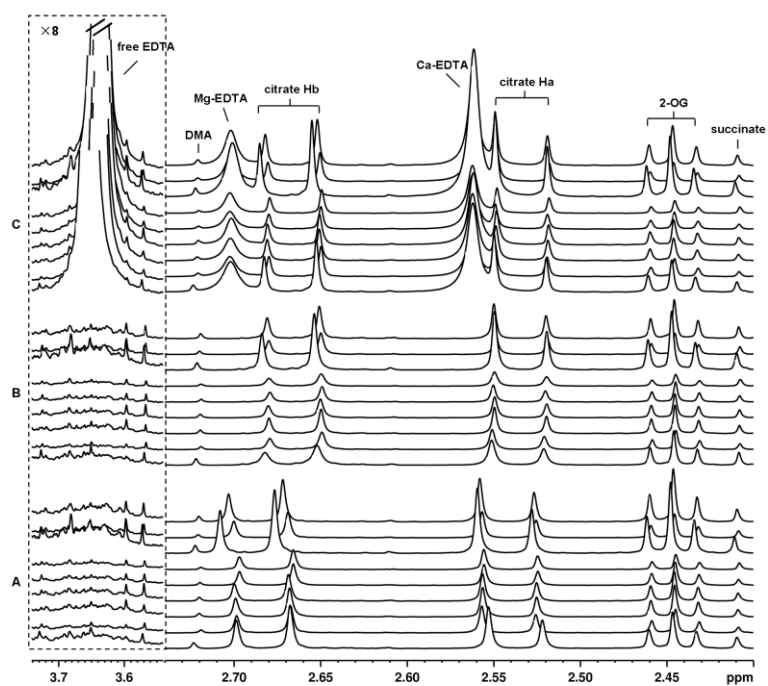


Fig. S8 ^1H NMR spectra (δ 2.40-2.74, δ 3.55-3.74) for rat urine samples ($n=9$) treated with phosphate buffer (A), with KF reaching final concentration of 159.5 mM KF followed with phosphate buffer (B) and with K_3EDTA reaching final concentration of 31.9 mM followed with phosphate buffer (C).

Fig. S9

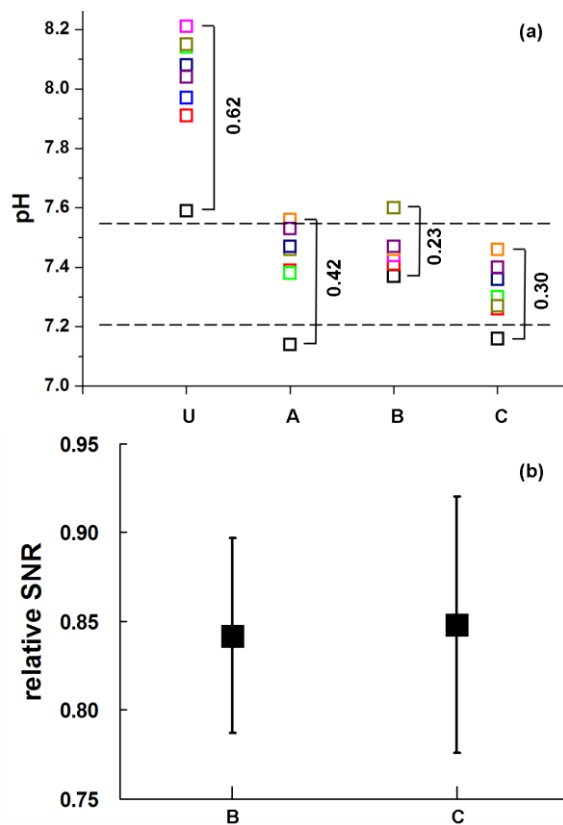


Fig. S9 Effects of sample treatments on sample pH (a) and signal-to-noise ratio (SNR) (b) for rat urine samples ($n=9$) which was calculated from the signal region of δ 2.42-2.47 (γ -CH₂ signal of 2-oxoglutarate) and noise region from δ -2 to δ -5. SNR data were normalized to that from samples treated with only phosphate buffer (mean \pm sd). U: with no treatment; A-C were same as in Figure S8.

Fig. S10

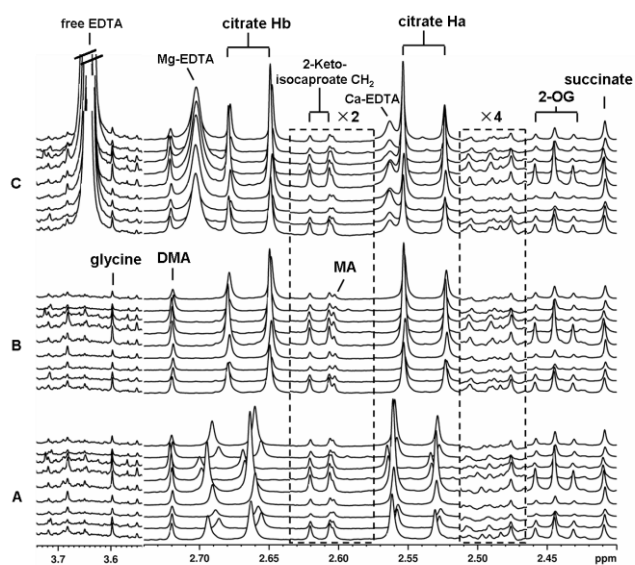


Fig. S10 ^1H NMR spectra (δ 2.40-2.74, δ 3.55-3.74) for mouse urine samples ($n=9$) treated with phosphate buffer (A), with KF reaching final concentration of 71.6 mM followed with phosphate buffer (B) and with K_3EDTA reaching final concentration of 7.2 mM followed with phosphate buffer (C).

Fig. S11

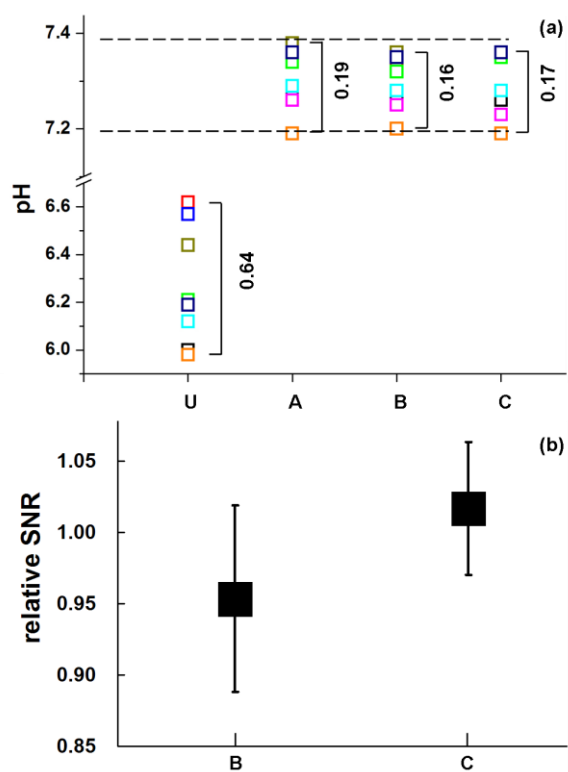


Fig. S11 Effects of sample treatments on sample pH (a) and signal-to-noise ratio (SNR) (b) for mouse urine samples (n=9) which was calculated from the signal region of δ 3.26-3.29 (CH_3 signal of TMAO) and the noise region was δ -2 to δ -5. SNR data were normalized to that from samples treated with only phosphate buffer (mean \pm sd). U: with no treatment; A-C were same as in Figure S10.

Fig. S12

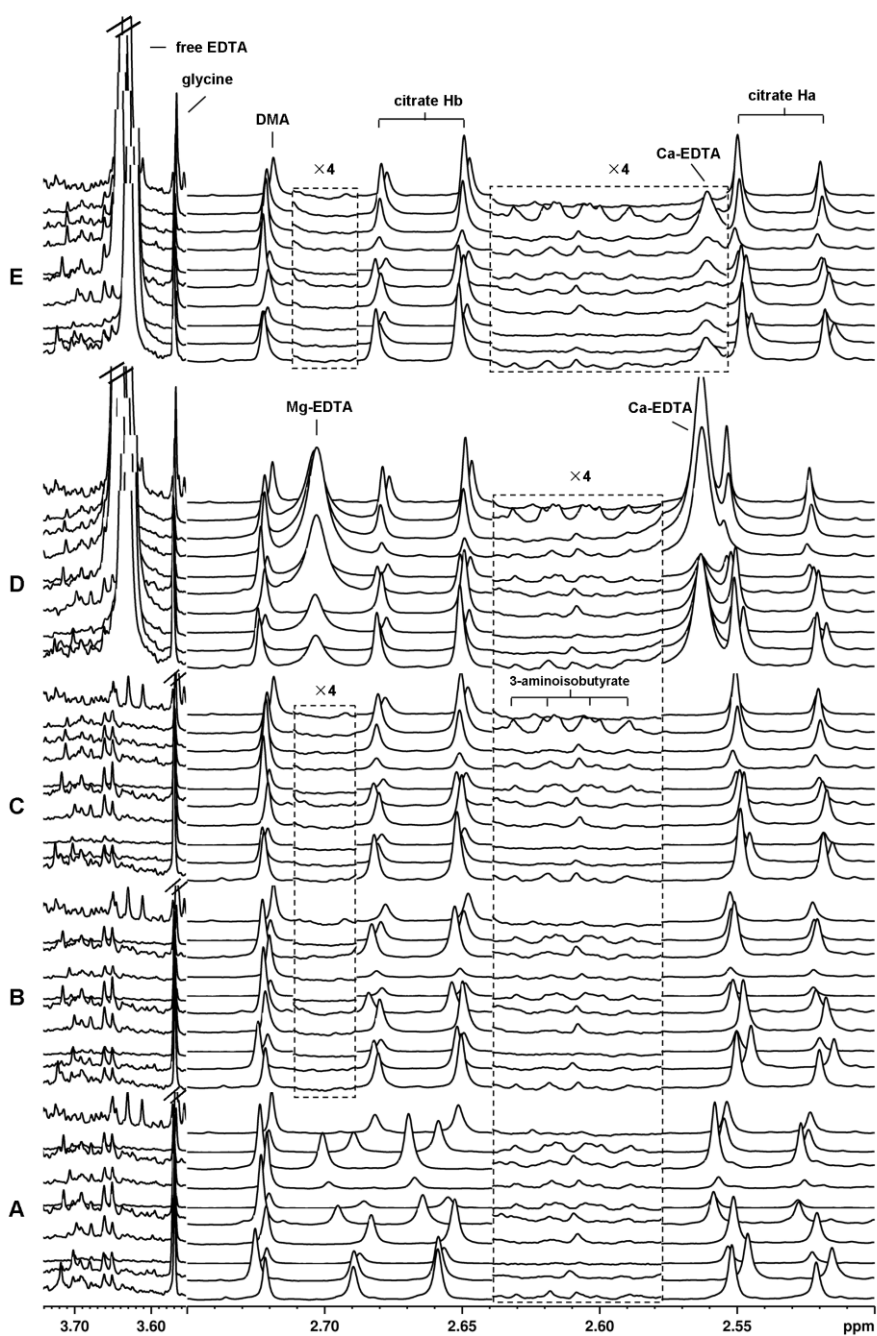


Fig. S12 ¹H NMR spectra (δ 2.50-2.75, δ 3.55-3.74) for human urine samples ($n=10$) treated with phosphate buffer (A), with KF reaching final concentration of 81.2 mM followed with phosphate buffer (B), with KF reaching final concentration of 120.7 mM followed with phosphate buffer (C), with K₃EDTA reaching final concentration of 13.0 mM followed with phosphate buffer (D) and with KF reaching final concentration of 120.7 mM followed with phosphate buffer and with K₃EDTA reaching final concentration of 6.0 mM (E). These 10 human urine samples were from nine adults and one 14-day-old new born baby.

Fig. S13

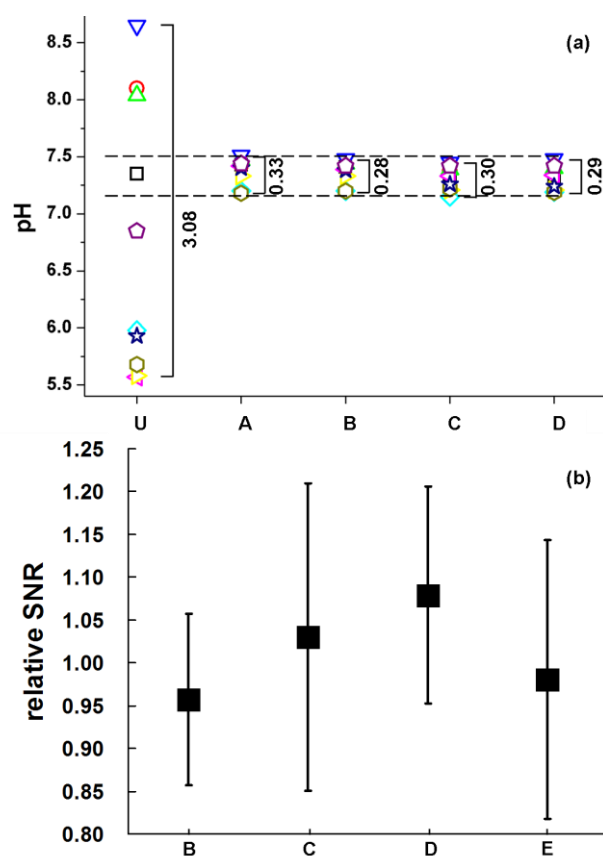


Fig. S13 Effects of sample treatments on sample pH (a) and signal-to-noise ratio (SNR) (b) for human urine samples (n=10) which was calculated from the signal region of δ 3.00-3.10 (CH_3 signal of creatinine) and the noise region was δ -2 to δ -5. SNR data were normalized to that from samples treated with only phosphate buffer (mean \pm sd). U: with no treatment; A-E were same as in Figure S12.

Fig. S14

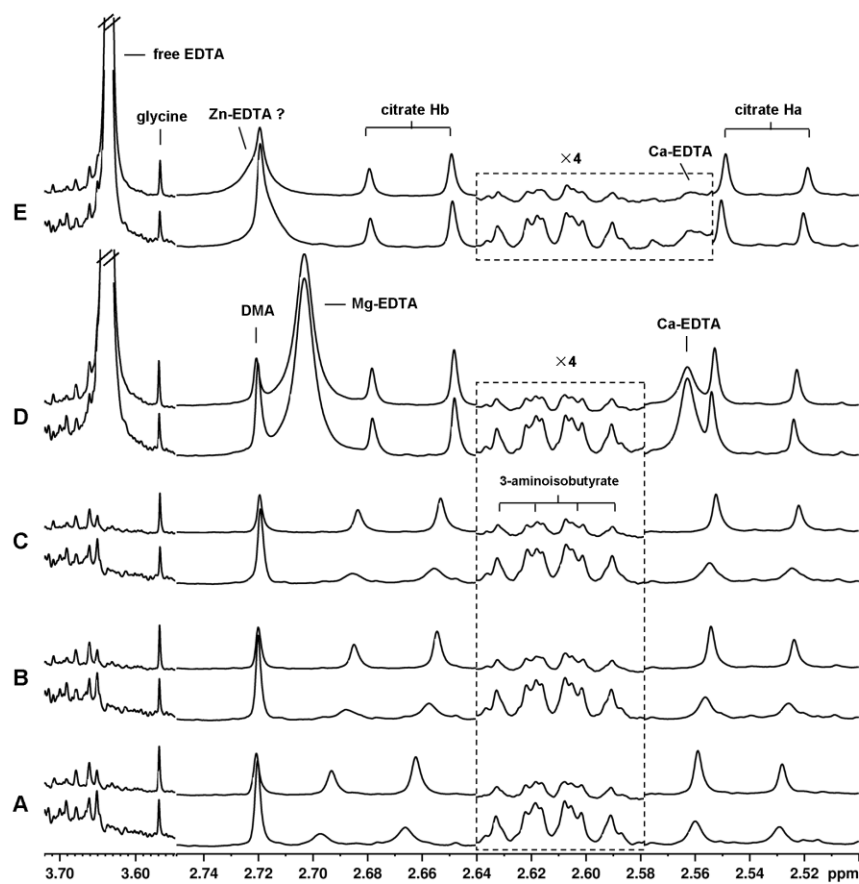


Fig. S14 ¹H NMR spectra (δ 2.50-2.75, δ 3.50-3.72) for one 28-month-old baby and one 5-month-old baby, A-E were same as in Figure S12.

Fig. S15

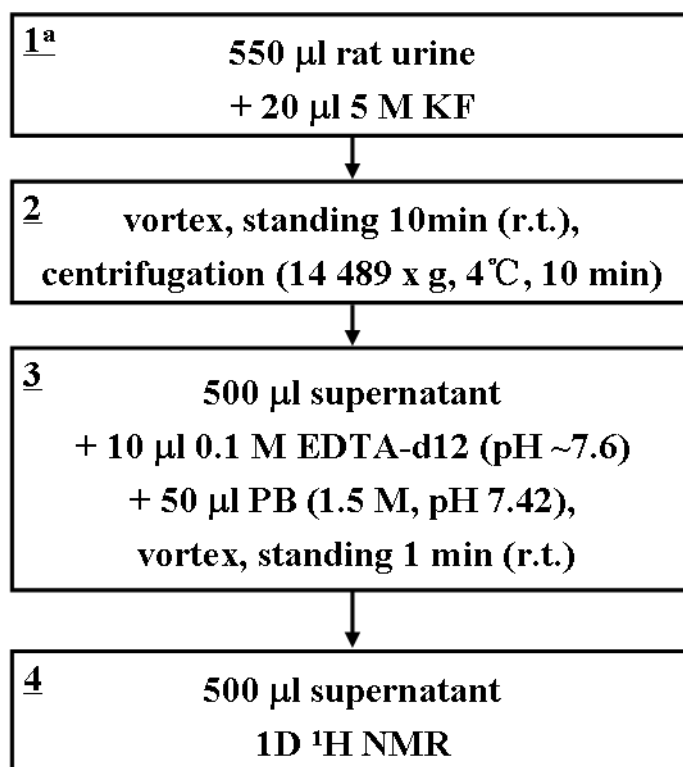


Fig. S15 Schematic flow chart for the improved urine sample preparation protocol based on KF addition (using rat urine as examples). PB, phosphate buffer. ^a details are described in the validation section for different urines.

Fig. S16

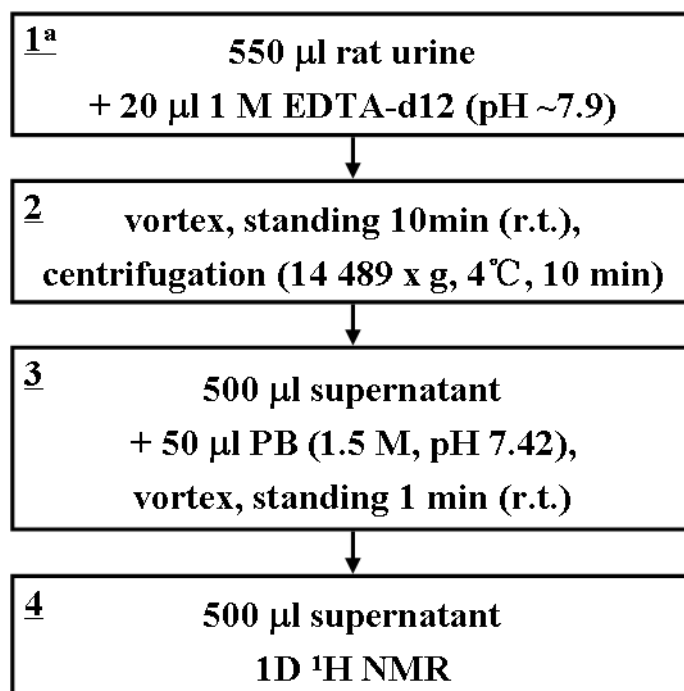


Fig. S16 Schematic flow chart of improved urine sample preparation methods using EDTA-d12 chelation. PB, phosphate buffer. ^a details are described in the validation section for different urines.